Language-Guided Salient Object Ranking (Supplementary Material)

Fang Liu Yuhao Liu Ke Xu Shuquan Ye Gerhard Petrus Hancke Rynson W.H. Lau
Department of Computer Science, City University of Hong Kong
{fawnliu2333, yuhaoLiu7456, kkangwing, shuquanye}@gmail.com
{gp.hancke, Rynson.Lau}@cityu.edu.hk

In Supp. A, we first elaborate on the implementation details of other methods to establish a basis for comparison. We then provide a detailed implementation of our method, including loss function, text parsing, and text encoder. Next, in Supp. B, we compare the computational costs of the different methods. In Supp. **??**, we compare the proposed method with other graph-based SOR approaches. In Supp. C, we ablate the effects of the number of graph convolution layers, the number of rank decoder layers, sentence features from different sources, and so on. Finally, in Supp. D, we present additional visual results.

A. Implementation Details

Implementations of Other Methods. For the salient instance/object detection methods [8, 19], we use the average saliency intensity to calculate the saliency ranks, following the method described in [13]. For instance segmentation methods [3, 9, 24], we modify the output layers to correspond with rank numbers from saliency ranking datasets and reinterpret category labels as rank labels.

For the large vision-and-language model-based method GiT [23], we adopt their instance segmentation setting, which adapts the window-based ViT [7, 14] to predict instance masks as a 1D sequence in raster order using an auto-regressive decoding paradigm. The number of output classes is adjusted according to the ranks of the two standard ranking datasets. A response example for instance segmentation in a sub-region of the input image is formatted as: $\{\langle\text{image}\rangle\langle\text{local feature}\rangle$ *"instance segmentation"* : $\langle\text{c}\rangle\langle\text{x}_1\rangle \langle y_1\rangle \dots \langle x_n\rangle\langle y_n\rangle\}$, where $\langle c\rangle$ is the class (rank) label, and $\langle x_1\rangle\langle y_1\rangle \dots \langle x_n\rangle\langle y_n\rangle$ represent the *n* offsets of the predicted mask in the corresponding sub-region.

For the language-guided segmentation method (*i.e.*, X-Decoder [28]), we input the same detailed text descriptions as ours, generated by [4] and capped at 256 tokens. After extracting visual and language features using Focal-T [27] for images and BERT [6] for texts, the X-Decoder concatenates the language features with visual query embeddings and feeds them into transformer decoder layers for cross-modal feature fusion. The output layer of the X-Decoder is modified to meet the specific requirements of the two saliency ranking benchmarks.

For a fair comparison, backbone of instance segmentation methods [3, 9, 23, 24] and language-guided segmentation method [28] are also pretrained on MS-COCO [15].

More Implementation Details. We employ both binary cross-entropy loss and dice loss [16] for supervising salient instance mask predictions. They are denoted as $\mathcal{L}_{mask} = \lambda_{ce}\mathcal{L}_{ce} + \lambda_{dice}\mathcal{L}_{dice}$, where the coefficients λ_{ce} and λ_{dice} are both set to 5.0. For the rank predictions, we utilize ranking loss [18], denoted as $\mathcal{L}_{rank}$. The overall training loss is therefore: $\mathcal{L} = \mathcal{L}_{mask} + \lambda_{rank}\mathcal{L}_{rank}$, where λ_{rank} is empirically set as 2.0. Our framework is based on Detectron2 [25] and requires approximately one day to converge on eight A100 GPUs.

Text Parsing. To get the object and relation phrases, we use spaCy [1] to extract all noun and relation phrases from input descriptions. Subsequently, we filter out the pronouns (*e.g.*, she, he, it), atmosphere words (*e.g.*, a soft or cozy atmosphere), and non-instance phrases (*e.g.*, game, environment, street, city). If noun or relation phrases repeat, we retain only the first occurrence of each phrase.

Text Encoder. For the input description, we first tokenize it into 256 tokens. We truncate the tokenized text to 256 tokens if it exceeds this length, or pad it to meet this size if it is shorter. Additionally, we insert two special tokens: a [CLS] token at the start and a [SEP] token at the end of the description. We then feed this tokenized description into BERT [6] ("bert-base-uncased") to obtain the corresponding output word embeddings. The output from the [CLS] token, designed to capture the context of the entire input description, is used as the sentence features for the input textual description. In the training process, we freeze the text encoder to stabilize the optimization process.

B. Computational Analysis

Computational Analysis of Different Methods. In Table A1, we compare the FLOPs, parameters, inference speed, and performances of different methods on ASSR test set [20]. While utilizing LVLM-generated descriptions for SOR, our

Table A1. Comparisons of FLOPs, Parameters, and Runtime of different methods. '-' denotes the results are not available. FLOPs are calculated for an input size of 1024×1024. Inference speed is tested on a single 4090 GPU.

Methods	Reference	Backbone	FLOPs ↓	Parameters ↓	Runtime ↓	SA-SOR ↑	SOR ↑	MAE ↓
GiT [23]	[ECCV'24]	GiT-B	-	158.74M	1398ms	0.541	0.854	0.101
OCOR [22]	[CVPR'22]	Swin-L	901.17G	401.67M	115ms	0.594	0.875	0.101
QAGNet [5]	[CVPR'24]	Swin-L	1007.79G	218.81M	289ms	0.772	0.867	0.052
DSGNN [26]	[CVPR'24]	Swin-L	703.15G	250.21M	325ms	0.765	0.860	0.051
PoseSOR [11]	[ECCV'24]	Swin-L	1524.36G	220.13M	581ms	0.664	0.854	0.077
Ours	-	Swin-L	1559.56G	327.03M	453ms	**0.787**	**0.895**	**0.049**

method performs better at the cost of acceptable computational overheads. Our approach (including the LVLM generation) processes an image in 453 ms, outperforming existing methods with a moderate inference cost.

Compared to GiT [23], which predicts masks and ranks as a 1D sequence in a time-consuming autoregressive manner, the proposed (Swin-L-based) method leverages LVLM-generated descriptions to achieve significantly better performance (SA-SOR: 44.18%; SOR: 4.92%; MAE: 54.46%) while being approximately 12× faster. Notably, despite processing text input, our approach achieves 1.6× faster inference speeds than DSGNN [26] while delivering better performance, with a 4.19% improvement in the SOR metric.

Computation Analysis of Different LVLMs. As our method uses the LVLM-generated descriptions to assist the SOR task, we report the computational costs of different LVLMs in Table A2. We use InstuctBLIP [9] as the default LVLM, as it is very efficient, and our method is robust to descriptions generated by different LVLMs (Table 4 in our paper).

Table A2. Computation costs of different LVLMs.

LVLMs	LLaVa [17]	OPERA [12]	GPT-4V [2]	InstructBLIP [4]
Parameters ↓	3.81G	7.91G	1.7T	7.91G
Runtime ↓	1.89s	12.21s	≈7s	0.33s

Computation Analysis of Different Components. We further report the computational costs of different components of our model based on the ResNet-50 backbone in Table A3. Although introducing the TGVM and TAVR modules increases the computational overheads, they are essential for enhancing the performance of our model.

Table A3. Computation costs of each component in our method (using ResNet-50 as the backbone).

Settings	TGVM	TAVR	FLOPs ↓	Parameters ↓	SA-SOR ↑
I			77.52G	153.50M	0.687
IV	✓		102.72G	154.29M	0.713
VIII	✓	✓	139.44G	155.41M	**0.733**

C. Additional Ablations

Number of Graph Convolution Layers. In Table A4, we study the effect of varying the number of graph convolution layers. The results show that increasing the number of layers (*e.g.*, from 1 to 2) enhances the model's reasoning ability, but adding too many layers (*e.g.*, 3) does not boost all metrics (with SOR being higher but SA-SOR and MAE worse). This may be attributed to the lengthy descriptions generated by LVLMs, where extra layers may over-complicate the model's inference, introducing noise that negatively impacts the performance. Thus, we choose two graph convolution layers for our model.

Table A4. Ablation study of the number of graph convolution layers used in TAVR.

Layers	SA-SOR ↑	SOR ↑	MAE ↓
1	0.714	0.876	0.066
2	**0.733**	0.882	**0.065**
3	0.731	**0.883**	0.065

Number of Rank Decoder Layers. Table A5 illustrates the impact of varying the number of rank decoder layers. The results show that using three layers yields the best performance across three metrics, surpassing both the single-layer and six-layer setups. Thus, we have selected three layers as the optimal configuration for our rank decoder.

Table A5. Ablation study of number of rank decoder layers.

Layers	SA-SOR ↑	SOR ↑	MAE ↓
1	0.716	0.865	0.068
3	**0.733**	**0.882**	**0.065**
6	0.728	0.880	0.066

Different Sentence Features from Text Encoder. In Table A6, we explore a variant where sentence features $\mathbf{L}_s$ are derived by averaging features from individual word tokens instead of using the [CLS] token, denoted as [CLS] → Words. The results indicate that representing sentence features with pooled word embeddings adversely affects performance. This validates that the [CLS] token more effectively

captures the global context of the entire input textual description.

Table A6. Ablation study of different sentence features.

Sentence Features	SA-SOR ↑	SOR ↑	MAE ↓
[CLS]	**0.733**	**0.882**	**0.065**
Words	0.729	0.880	0.066

Discussion on TAVR. We visualize the activation map for different relation phrases of TAVR in Fig. A1, which shows that TAVR can locate the corresponding objects for different relation phrases, facilitating the SOR task.

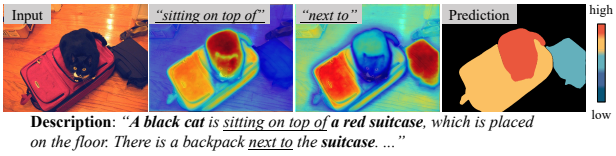

Figure A1. Visualization of the activation map for different relation phrases of TAVR.

Ablation Study of Wrong Description. To further test our model, we deliberately feed completely wrong descriptions (using descriptions generated for other images) with the target images to our model. For example, we randomly sample one description and treat it as a completely wrong description for all target images. The results (denoted as "Wrong Descriptions") are shown in Table A7, which indicates that using completely wrong descriptions indeed harms the model's performance. This is expected, as the erroneous text describes another image, which is unrelated to the corresponding target images. However, since visual features are still used in our approach, our model can utilize visual features to aid in ranking and mitigate the negative effects of incorrect input descriptions, thus achieving comparable performance to other methods.

Table A7. Ablation study of different descriptions.

Captions	SA-SOR ↑	SOR ↑	MAE ↓
Wrong Descriptions	0.668	0.847	0.075
Ours	**0.733**	**0.882**	**0.065**

Visual Comparisons of Introducing Language Description. Fig. A2 illustrates the effectiveness of incorporating language descriptions into saliency ranking. The second column shows the model's results without descriptions, where both TGVM and TAVR modules are removed, and we directly input the multiscale visual features into the transformer decoder to generate the ranking predictions. The visual results demonstrate that our approach effectively leverages the rich semantic information (*e.g.*, salient objects and their relations) of textual descriptions to enhance saliency ranking. For example, in the first row, the model without using the description erroneously highlights only the most salient object (*'the cat'*), but our method ranks *'the cat'* as the most salient and *'a chair'* as the second simultaneously, aligning with their orders in the description. The second row presents a more complex scenario. Unlike the model without descriptions, which only identifies the most salient object, our approach accurately recognizes *'a woman'* and *'a surfboard'* as the most and second salient objects, respectively, before shifting focus to *'a small dog'* and *'other surfboards'*. This capability stems from our method's effectiveness in extracting valuable information from the multimodal graph, utilizing implicit orders and relationships (*e.g.*, *'standing on'* and *'sitting on'*) detailed in the textual description.

D. More Visual Results

We present the comparison of our method against the eleven top-performing methods listed in Table 1, as shown in Fig. A3 – A8. These methods include Mask2Former [3], GiT [23], X-Decoder [28], ASSR [20], IRSR [18], OCOR [22], PSR [21], SeqRank [10], QAG-Net [5], DSGNN [26], and PoseSOR [11].

Fig. A3 – A5 demonstrate that our model effectively ranks salient objects based on their implicit orders in the description. For instance, the first row of Fig. A3 shows our model prioritizing *'a man'* and *'a wooden bench'* over *'a boat in the water'*, following the implicit narrative sequence in the description. Similarly, in first row of Fig. A4, the model identifies *'a man'* and *'a magazine with a picture of a woman on the cover'* as the most and second-most salient objects, respectively, with *'a refrigerator'* ranked third. Even when background elements such as *'a sink'* and *'a clock'* are present, our approach effectively extracts useful information from the language description and suppresses these distractions. These results further validate that our method can decipher the implicit orders of salient objects from textual descriptions while effectively minimizing background noise.

Furthermore, our method exhibits robustness in capturing saliency by effectively deciphering positional context and object relationships, even when the order in the language description does not precisely align with the ground truth, which is demonstrated in Fig. A6 – A8. For example, the third row of Fig. A6 initially describes *'a woman'*, *'a baby'* then *'a white stuffed teddy bear'*. But, according to the ground truth, *'a baby'* should be the most salient. Despite this, our approach successfully utilizes relationships (*e.g.*, *'holding'* and *'being enjoyed while held'*) and the entity phrases to construct a multimodal graph, enhancing the model's reasoning for the salient objects' ranking orders. In the last row of Fig. A7, our method effectively learns the positional context from the multimodal graph by integrating

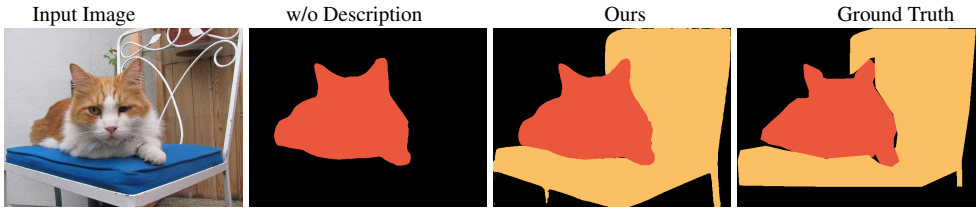

Description: "***An adorable orange and white cat*** *is resting on* ***a blue cushion*** *placed on* ***a white chair***. ***The cat*** *appears to be relaxed and comfortable as it lounges on the cushion, possibly enjoying the sunny outdoor setting.* ***The chair*** *is positioned in front of a potted plant, which adds a touch of greenery to the scene ...*"

Description: "***A woman*** *is standing on* ***a surfboard*** *in the middle of a body of water, holding a paddle. She is accompanied by* ***a small dog sitting on the surfboard*** *next to her. Both the woman and the dog appear to be enjoying their time on the water. There are several* ***other surfboards visible in the background***, *suggesting that there may be other people out on the water ...*"

Figure A2. The effectiveness of introducing language description for saliency ranking.

semantic textual information with visual features.

References

[1] spacy. https://spacy.io/. 1

[2] Josh Achiam, Steven Adler, Sandhini Agarwal, Lama Ahmad, Ilge Akkaya, Florencia Leoni Aleman, Diogo Almeida, Janko Altenschmidt, Sam Altman, Shyamal Anadkat, et al. Gpt-4 technical report. *arXiv:2303.08774*, 2023. 2

[3] Bowen Cheng, Ishan Misra, Alexander G Schwing, Alexander Kirillov, and Rohit Girdhar. Masked-attention mask transformer for universal image segmentation. In *CVPR*, 2022. 1, 3, 6, 7, 8, 9, 10, 11

[4] Wenliang Dai, Junnan Li, Dongxu Li, Anthony Meng Huat Tiong, Junqi Zhao, Weisheng Wang, Boyang Li, Pascale N Fung, and Steven Hoi. Instructblip: Towards general-purpose vision-language models with instruction tuning. In *NeurIPS*, 2023. 1, 2

[5] Bowen Deng, Siyang Song, Andrew P French, Denis Schluppeck, and Michael P Pound. Advancing saliency ranking with human fixations: Dataset models and benchmarks. In *CVPR*, 2024. 2, 3, 6, 7, 8, 9, 10, 11

[6] Jacob Devlin, Ming-Wei Chang, Kenton Lee, and Kristina Toutanova. Bert: Pre-training of deep bidirectional transformers for language understanding. *arXiv:1810.04805*, 2018. 1

[7] Alexey Dosovitskiy. An image is worth 16x16 words: Transformers for image recognition at scale. In *ICLR*, 2021. 1

[8] Ruochen Fan, Ming-Ming Cheng, Qibin Hou, Tai-Jiang Mu, Jingdong Wang, and Shi-Min Hu. S4net: Single stage salient-instance segmentation. In *CVPR*, 2019. 1

[9] Yuxin Fang, Shusheng Yang, Xinggang Wang, Yu Li, Chen Fang, Ying Shan, Bin Feng, and Wenyu Liu. Instances as queries. In *ICCV*, 2021. 1

[10] Huankang Guan and Rynson W.H. Lau. Seqrank: Sequential ranking of salient objects. In *AAAI*, 2024. 3, 6, 7, 8, 9, 10, 11

[11] Huankang Guan and Rynson WH Lau. Posesor: Human pose can guide our attention. In *ECCV*, 2024. 2, 3, 6, 7, 8, 9, 10, 11

[12] Qidong Huang, Xiaoyi Dong, Pan Zhang, Bin Wang, Conghui He, Jiaqi Wang, Dahua Lin, Weiming Zhang, and Nenghai Yu. Opera: Alleviating hallucination in multi-modal large language models via over-trust penalty and retrospection-allocation. In *CVPR*, 2024. 2

[13] Md Amirul Islam, Mahmoud Kalash, and Neil DB Bruce. Revisiting salient object detection: Simultaneous detection, ranking, and subitizing of multiple salient objects. In *CVPR*, 2018. 1

[14] Yanghao Li, Hanzi Mao, Ross Girshick, and Kaiming He. Exploring plain vision transformer backbones for object detection. In *ECCV*, 2022. 1

[15] Tsung-Yi Lin, Michael Maire, Serge Belongie, James Hays, Pietro Perona, Deva Ramanan, Piotr Dollár, and C Lawrence Zitnick. Microsoft coco: Common objects in context. In *ECCV*, 2014. 1

[16] Tsung-Yi Lin, Priya Goyal, Ross Girshick, Kaiming He, and Piotr Dollár. Focal loss for dense object detection. In *ICCV*, 2017. 1

[17] Haotian Liu, Chunyuan Li, Qingyang Wu, and Yong Jae Lee. Visual instruction tuning. In *NeurIPS*, 2023. 2

[18] Nian Liu, Long Li, Wangbo Zhao, Junwei Han, and Ling Shao. Instance-level relative saliency ranking with graph reasoning. *IEEE TPAMI*, 2021. 1, 3, 6, 7, 8, 9, 10, 11

[19] Nian Liu, Ni Zhang, Kaiyuan Wan, Ling Shao, and Junwei Han. Visual saliency transformer. In *ICCV*, 2021. 1

[20] Avishek Siris, Jianbo Jiao, Gary KL Tam, Xianghua Xie, and Rynson WH Lau. Inferring attention shift ranks of objects for image saliency. In *CVPR*, 2020. 1, 3, 6, 7, 8, 9, 10, 11

[21] Chengxiao Sun, Yan Xu, Jialun Pei, Haopeng Fang, and He Tang. Partitioned saliency ranking with dense pyramid transformers. In *ACM MM*, 2023. 3, 6, 7, 8, 9, 10, 11

[22] Xin Tian, Ke Xu, Xin Yang, Lin Du, Baocai Yin, and Rynson WH Lau. Bi-directional object-context prioritization learning for saliency ranking. In *CVPR*, 2022. 2, 3, 6, 7, 8, 9, 10, 11

[23] Haiyang Wang, Hao Tang, Li Jiang, Shaoshuai Shi, Muhammad Ferjad Naeem, Hongsheng Li, Bernt Schiele, and Liwei Wang. Git: Towards generalist vision transformer through universal language interface. In *ECCV*, 2024. 1, 2, 3, 6, 7, 8, 9, 10, 11

[24] Xinlong Wang, Rufeng Zhang, Tao Kong, Lei Li, and Chunhua Shen. Solov2: Dynamic and fast instance segmentation. In *NeurIPS*, 2020. 1

[25] Yuxin Wu, Alexander Kirillov, Francisco Massa, Wan-Yen Lo, and Ross Girshick. Detectron2. https://github.com/facebookresearch/detectron2, 2019. 1

[26] Zijian Wu, Jun Lu, Jing Han, Lianfa Bai, Yi Zhang, Zhuang Zhao, and Siyang Song. Domain separation graph neural networks for saliency object ranking. In *CVPR*, 2024. 2, 3, 6, 7, 8, 9, 10, 11

[27] Jianwei Yang, Chunyuan Li, Pengchuan Zhang, Xiyang Dai, Bin Xiao, Lu Yuan, and Jianfeng Gao. Focal attention for long-range interactions in vision transformers. In *NeurIPS*, 2021. 1

[28] Xueyan Zou, Zi-Yi Dou, Jianwei Yang, Zhe Gan, Linjie Li, Chunyuan Li, Xiyang Dai, Harkirat Behl, Jianfeng Wang, Lu Yuan, et al. Generalized decoding for pixel, image, and language. In *CVPR*, 2023. 1, 3, 6, 7, 8, 9, 10, 11

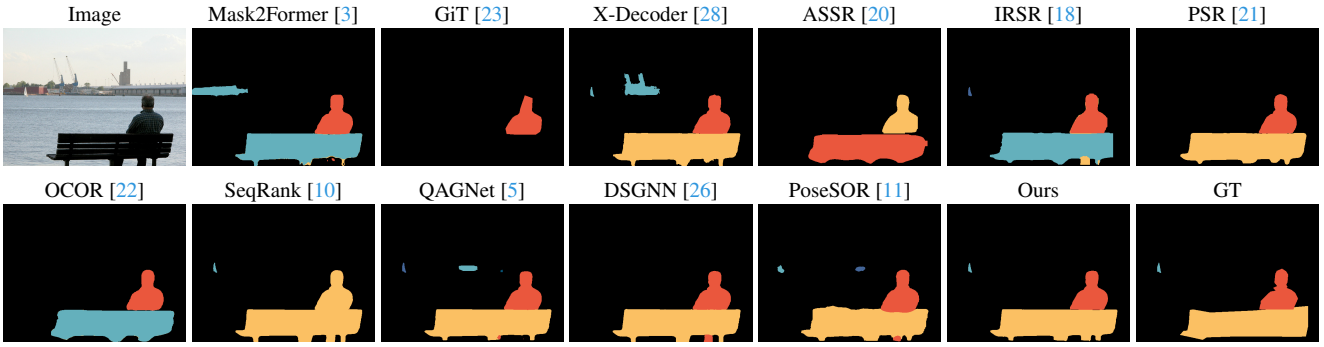

Description: "***A man*** *is sitting on* ***a wooden bench*** *near a body of water, possibly the ocean. He is wearing a plaid shirt and appears to be enjoying the view. The scene also includes* ***a boat in the water*** *and a crane in the background, ...*"

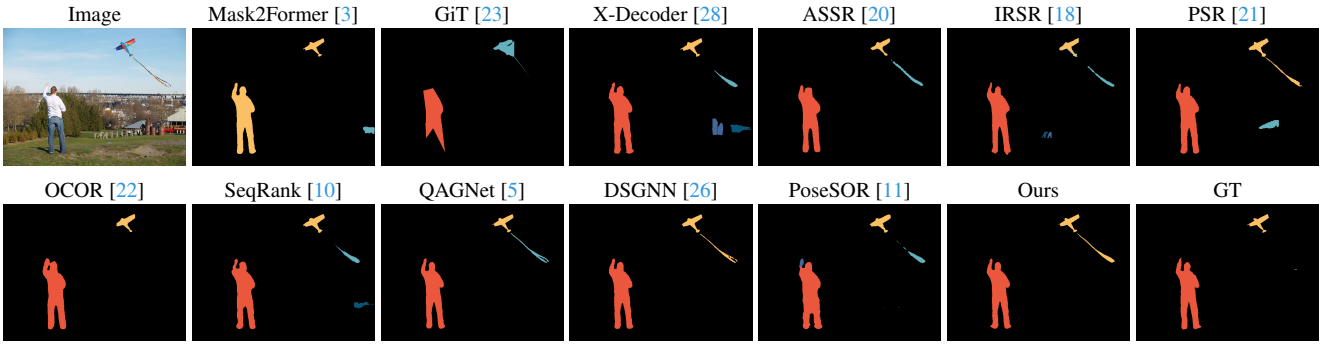

Description: "***A man*** *standing on a grassy field, flying* ***a colorful kite*** *in the sky. He is wearing a white shirt and appears to be enjoying the outdoor activity. In the background, there is a bridge spanning across the landscape, ...*"

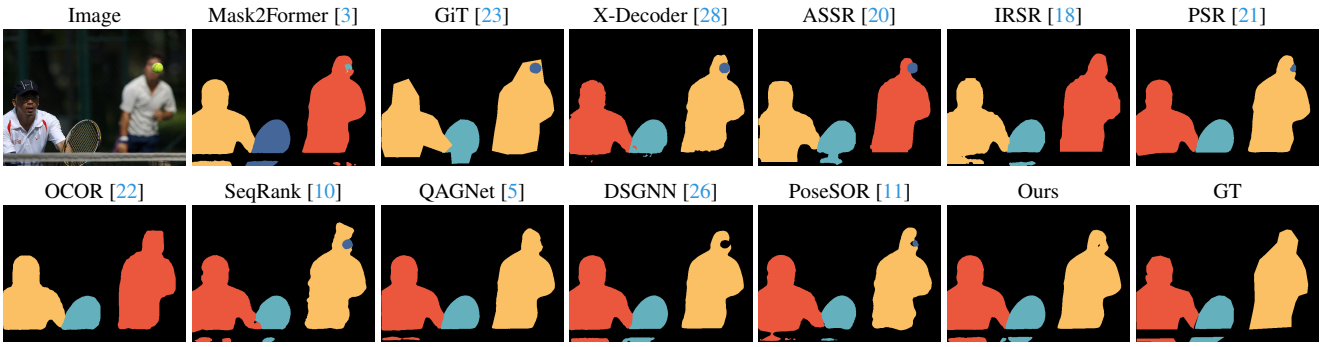

Description: "***Two men*** *are playing a game of tennis on a tennis court.* ***One of them*** *is holding* ***a tennis racket****, ready to hit the ball that is coming towards him.* ***The other man*** *is standing nearby, possibly waiting for his turn to hit the ball ...*"

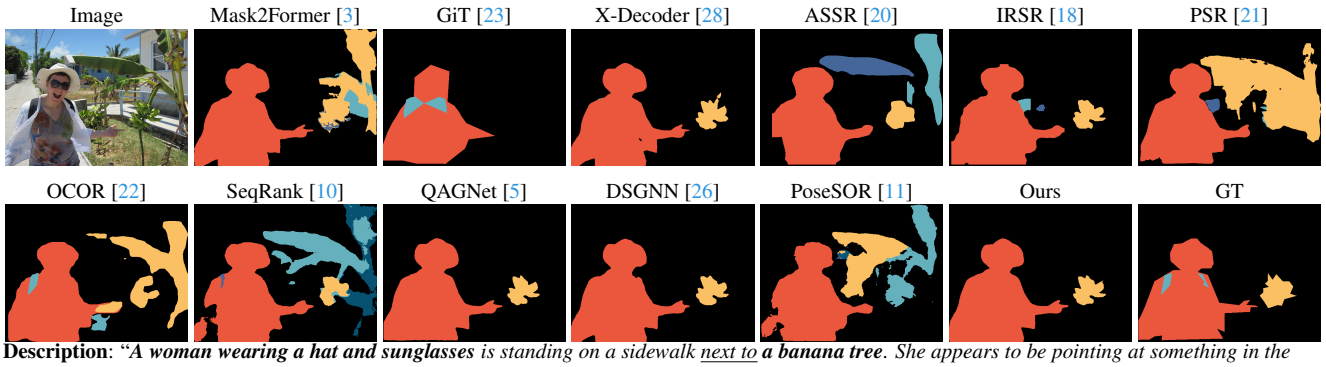

Description: "***A woman wearing a hat and sunglasses*** *is standing on a sidewalk next to* ***a banana tree****. She appears to be pointing at something in the distance, possibly enjoying the scenery around her. The banana tree is located towards ...*"

Figure A3. Qualitative comparison of our method with eleven best-performing methods in Table 1.

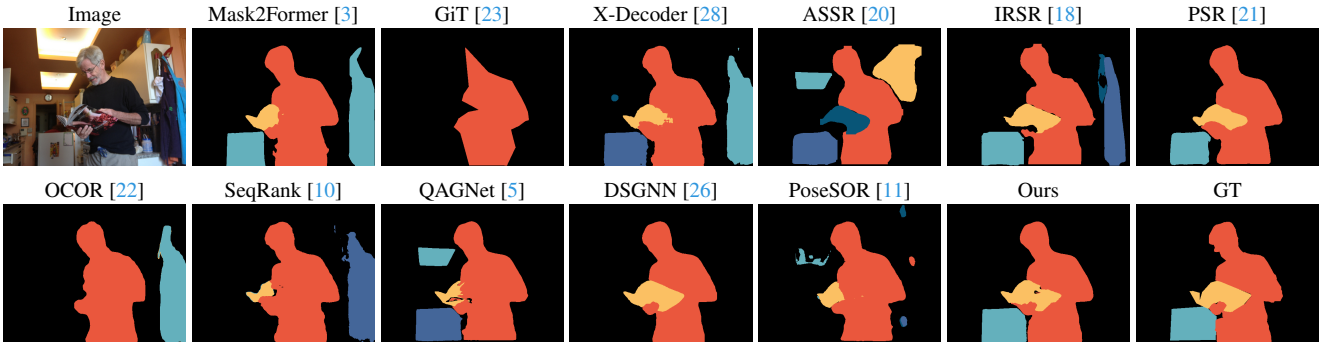

Description: "***A man*** *is standing in a kitchen, holding* ***a magazine with a picture of a woman on the cover****. He is wearing a black shirt and appears to be reading* ***the magazine****. The kitchen has* ***a refrigerator****, a sink, and a clock on the wall ...*"

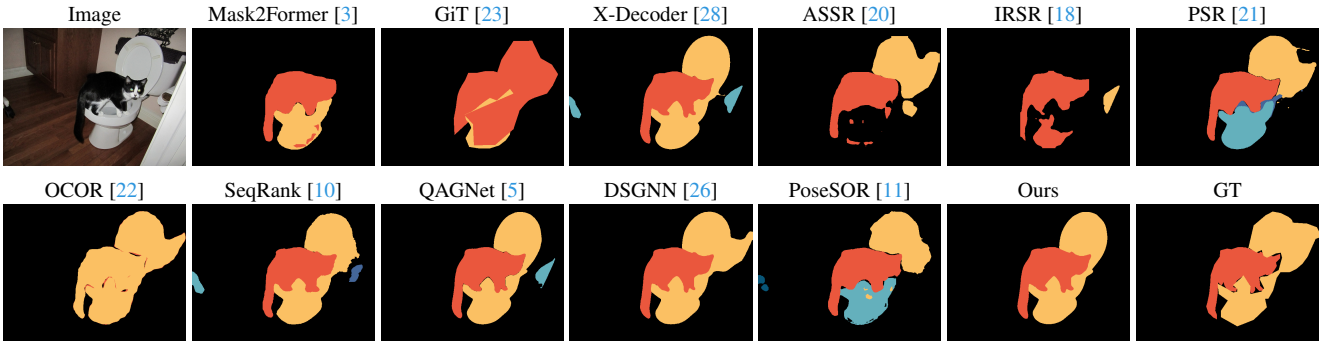

Description: "***A black and white cat*** *is standing on top of* ***a white toilet*** *in a bathroom. The cat appears to be enjoying its time on the toilet, as it seems to be licking its paw ...*"

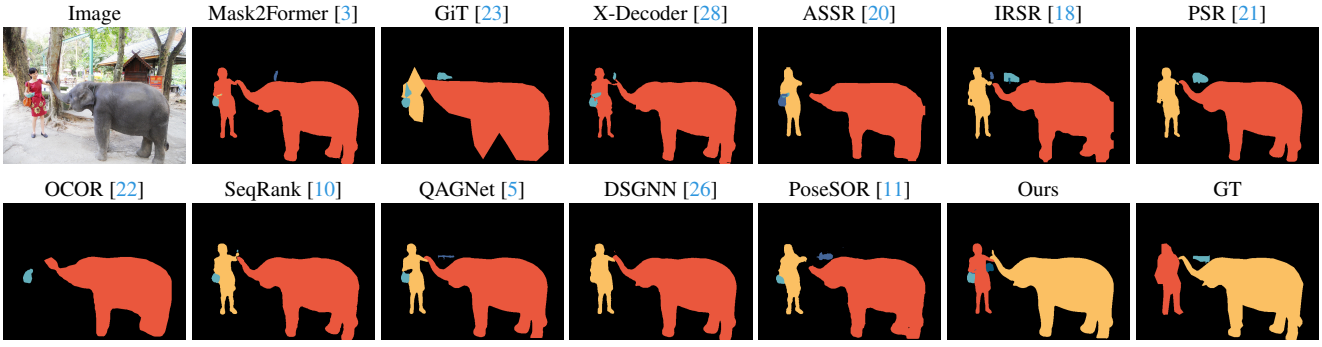

Description: "***A woman*** *is standing next to* ***a small elephant*** *in a dirt area. The elephant is reaching out its trunk towards the woman, who appears to be petting it. The elephant's trunk is touching the woman's hand, and she is smiling ...*"

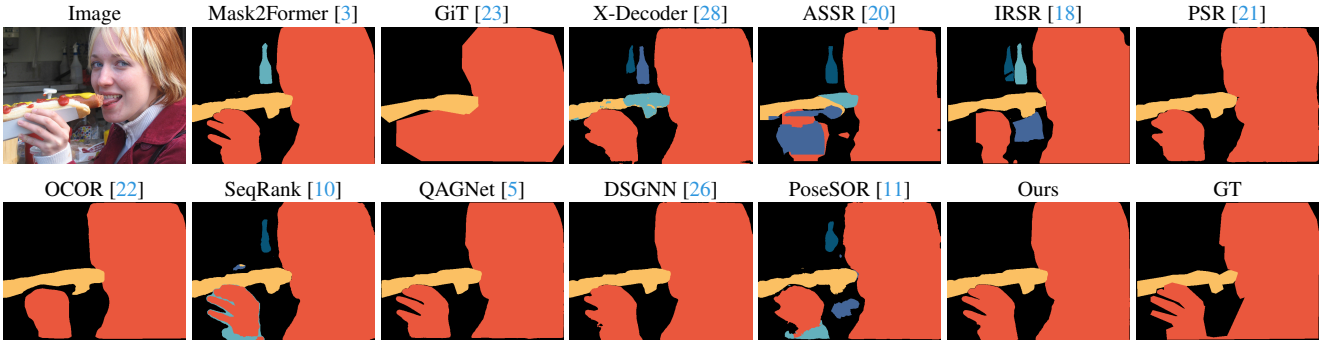

Description: "***A young woman*** *wearing a red jacket is biting into* ***a long hot dog*** *covered in mustard and ketchup. The hot dog appears to be quite large, taking up a significant portion of the woman's mouth. ...*"

Figure A4. Qualitative comparison of our method with eleven best-performing methods in Table 1.

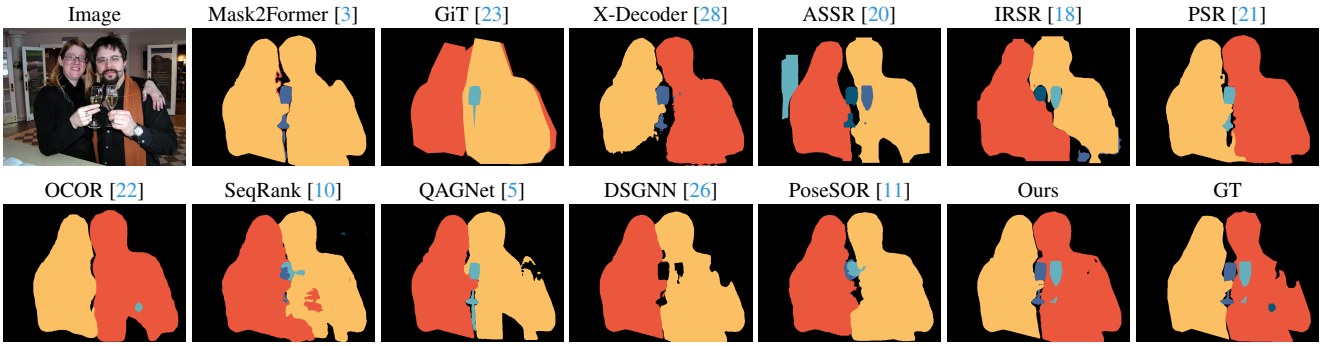

Description: "***A man*** *and* ***a woman*** *are standing together, holding* ***wine glasses*** *and posing for a picture. The man is wearing glasses and a scarf, while the woman is wearing a black shirt. They are both smiling ...*"

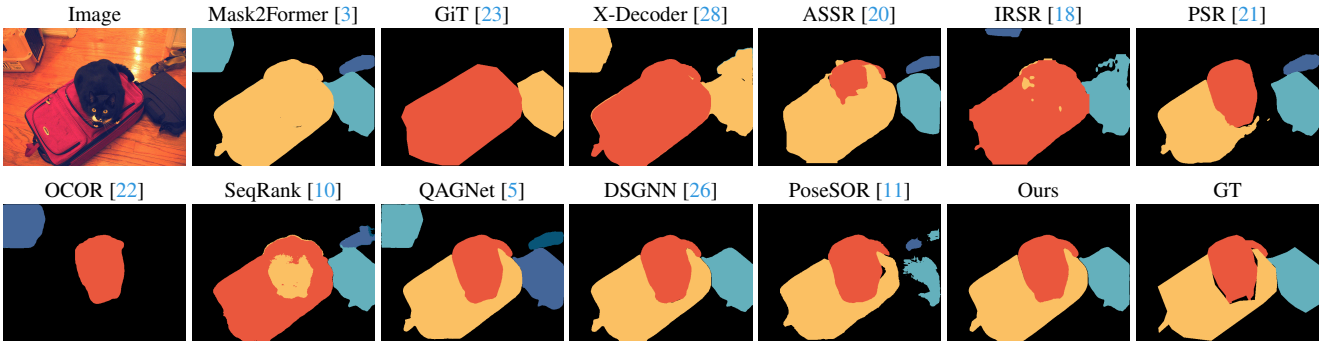

Description: "***A black cat*** *is sitting on top of* ***a red suitcase****, which is placed on the floor. The cat appears to be looking at the camera. There is a* ***backpack*** *next to the suitcase. The scene is set in a room with a wooden floor. ...*"

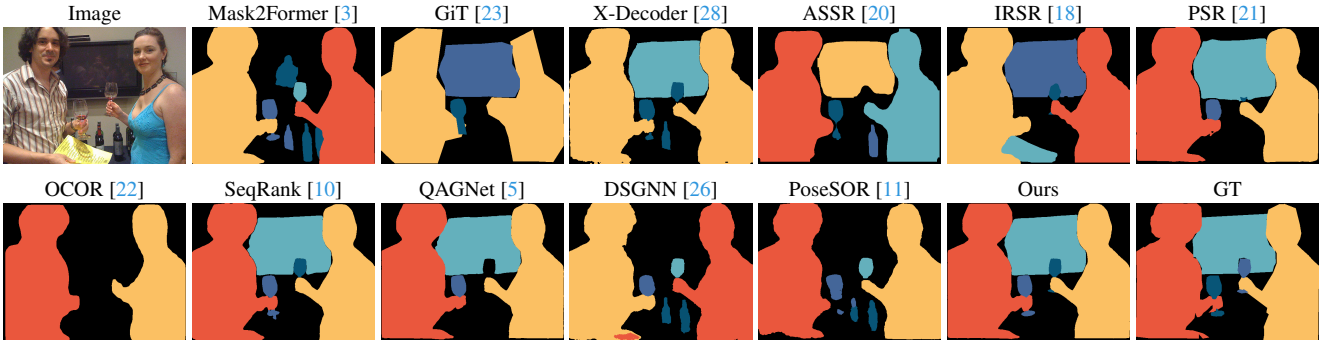

Description: "***A man*** *and* ***a woman*** *are standing together, holding* ***wine glasses****, and posing for a picture. They are surrounded by several wine bottles. The man is wearing a striped shirt, and the woman is wearing a blue dress ...*"

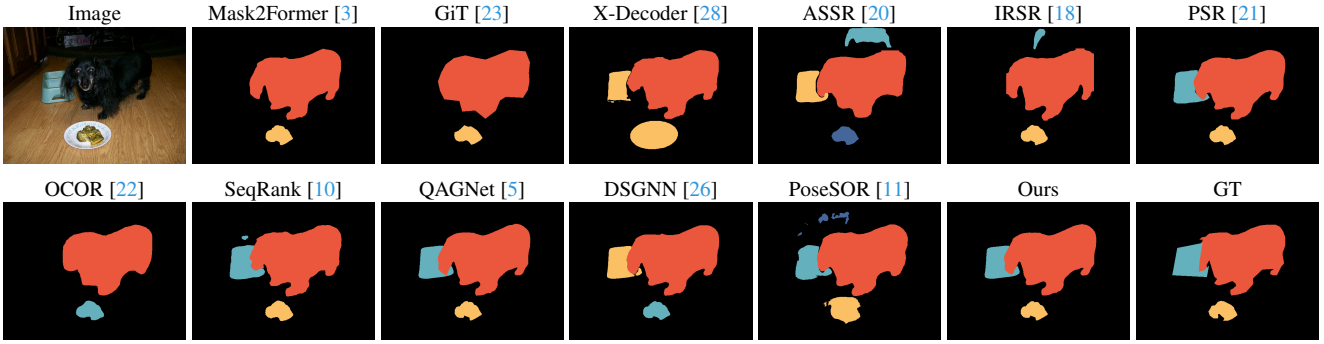

Description: "***A small black dog*** *is standing on a wooden floor next to* ***a white plate containing broccoli****. The dog seems to be curious about the broccoli and is staring intently at it. There are* ***a bowl*** *on the left side of the image ...*"

Figure A5. Qualitative comparison of our method with eleven best-performing methods in Table 1.

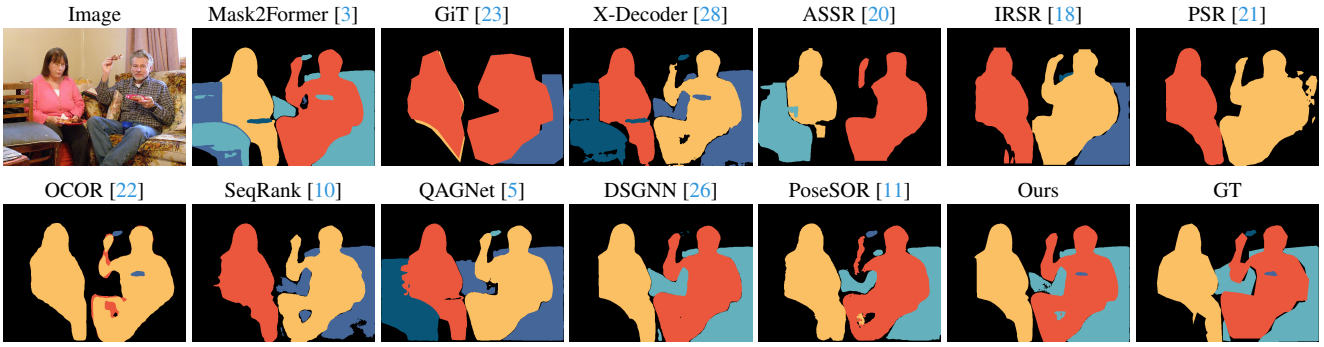

Description: "***A man*** *and* ***a woman*** *are sitting on* ***a couch***, *enjoying* ***pizza*** *together. The man is holding a slice of pizza in his hand, while the woman is also holding a slice. There are two pizza slices visible in the scene ...*"

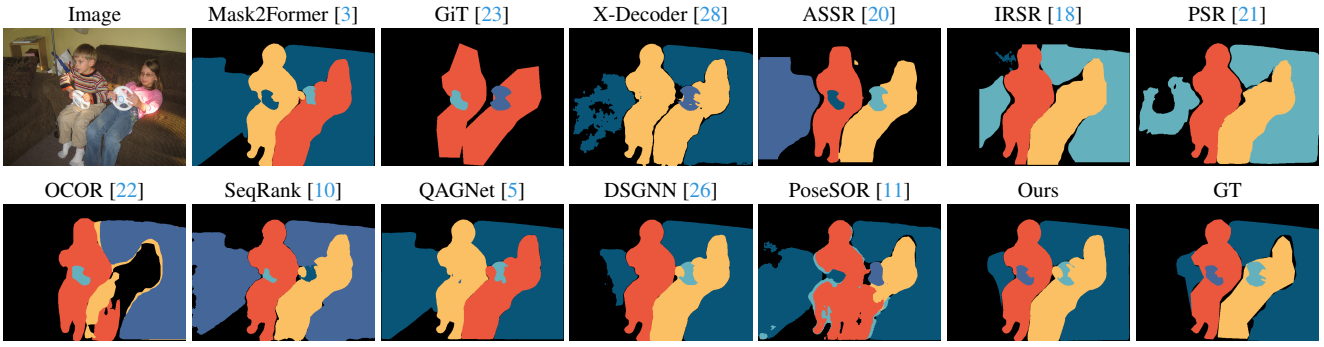

Description: "***A young boy*** *and* ***girl*** *are sitting on* ***a couch***, *playing a video game together. They are holding* ***Wii controllers*** *in their hands, fully engaged in the game. The room has a cozy atmosphere, ...*"

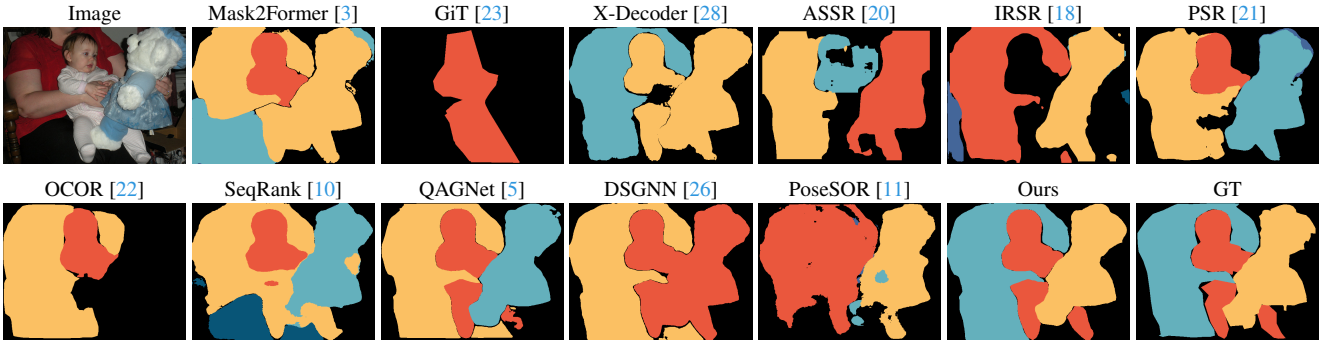

Description: "***A woman*** *is sitting in a chair and holding* ***a baby*** *close to her chest. The baby is wearing a pink outfit and appears to be enjoying being held by the woman. The woman is also holding* ***a white stuffed teddy bear*** *in her other hand. ...*"

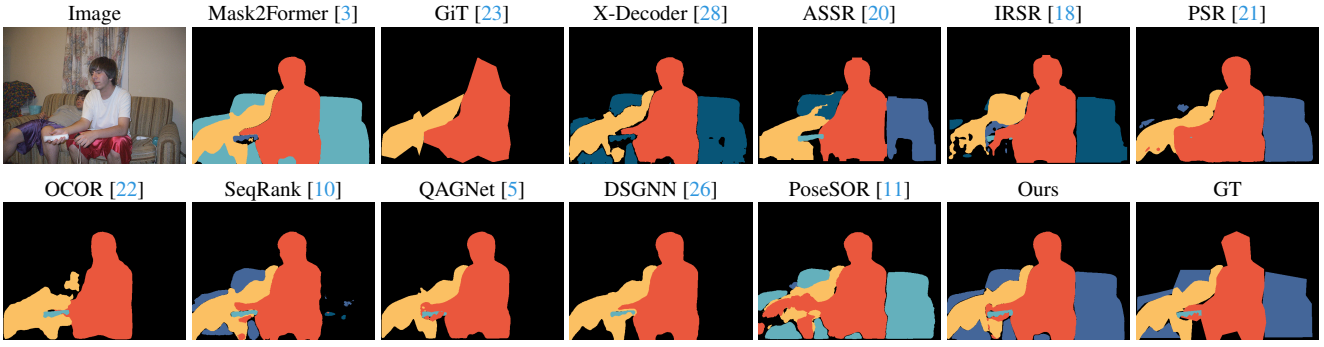

Description: "***Two young men*** *are sitting on* ***a couch***, *playing a video game together. One of the men is holding* ***a Wii remote***, *while the other is holding a Nintendo Wii controller. The couch is positioned against a wall, ...*"

Figure A6. Qualitative comparison of our method with eleven best-performing methods in Table 1.

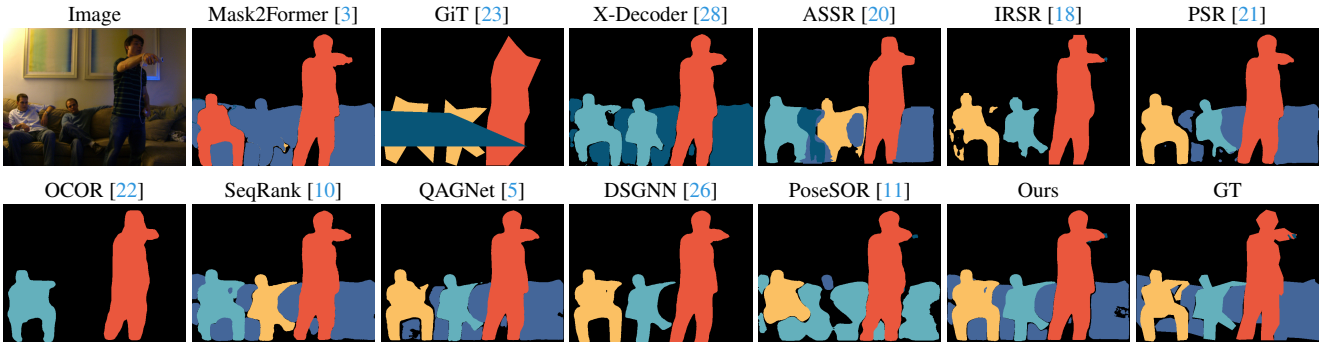

Description: *"A group of people gathered in a living room, playing a video game together.* ***A man*** *is holding* ***a Wii remote****, and playing a video game.* ***Other people*** *are sitting on* ***a couch****, watching the man play. The living room is furnished ..."*

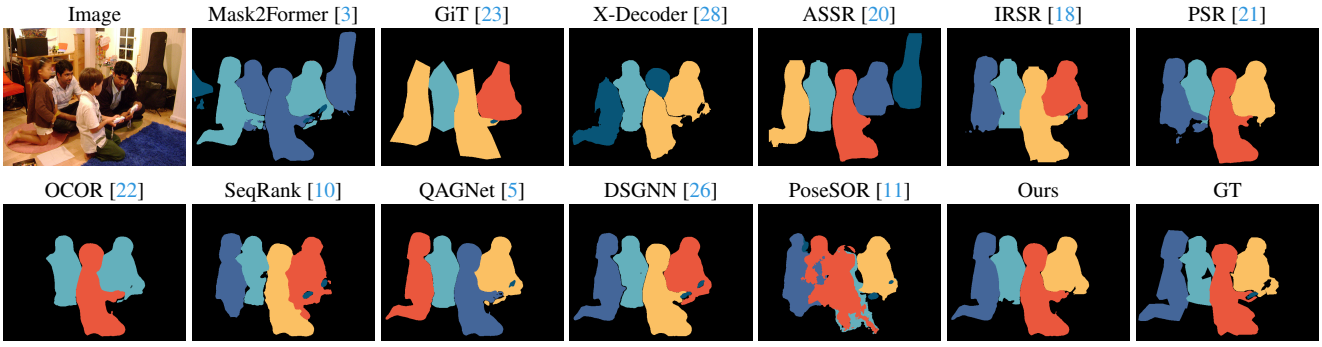

Description: "***A group of people*** *gathered in a living room, playing a video game together. Two adults and two children are sitting on the floor, all holding Nintendo Wii controllers. They appear to be enjoying the game ..."*

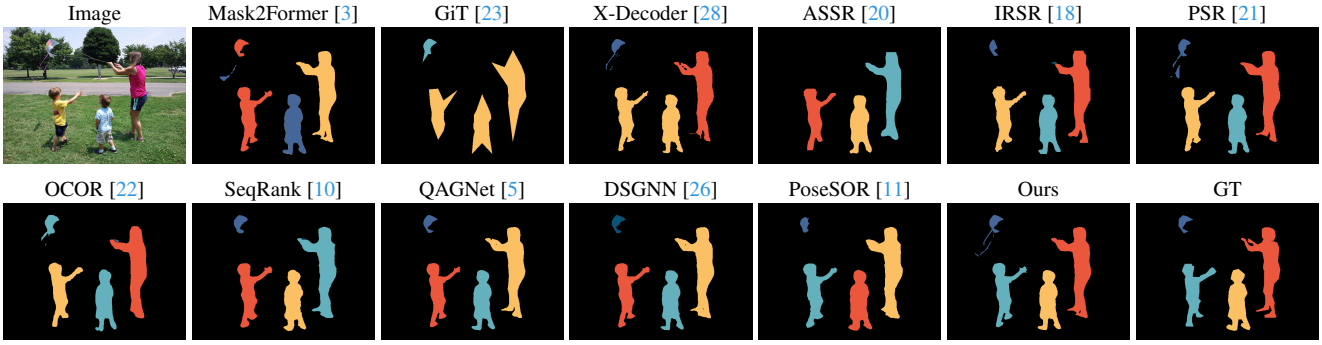

Description: "***A woman*** *and* ***two young boys*** *are playing with* ***a kite*** *in a park. The woman is holding the kite while the boys are standing next to her, looking up at the kite as it flies in the air. It appears to be a fun and enjoyable moment ..."*

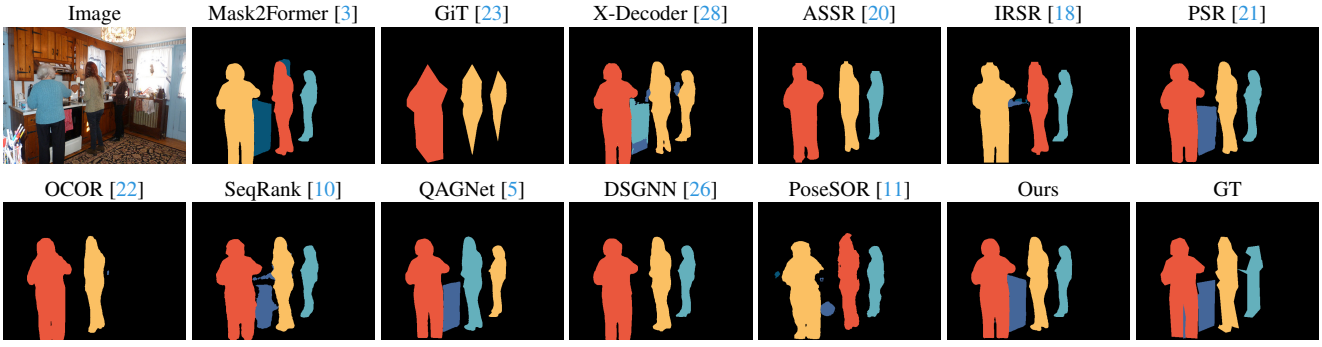

Description: "***A group of three women*** *are standing in a kitchen, preparing food and drinks.* ***Two of the women*** *are on the left side of the kitchen, while* ***the third woman*** *is on the right side. They appear to be engrossed in their tasks, ..."*

Figure A7. Qualitative comparison of our method with eleven best-performing methods in Table 1.

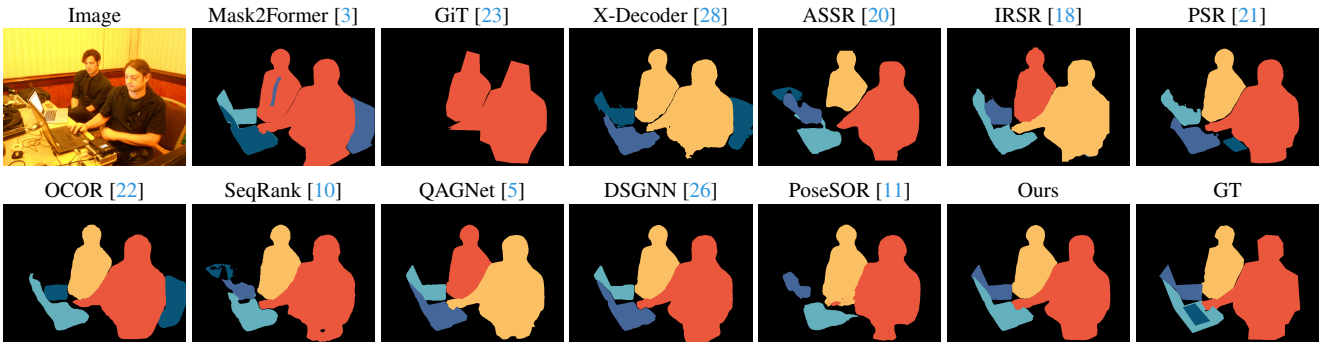

Description: "***Two men*** *are sitting at a desk, both wearing black shirts and ties. They are working on their* ***laptops***. ***One of the laptops*** *is positioned closer to the left side of the desk, while* ***the other one*** *is situated on the right side ...*"

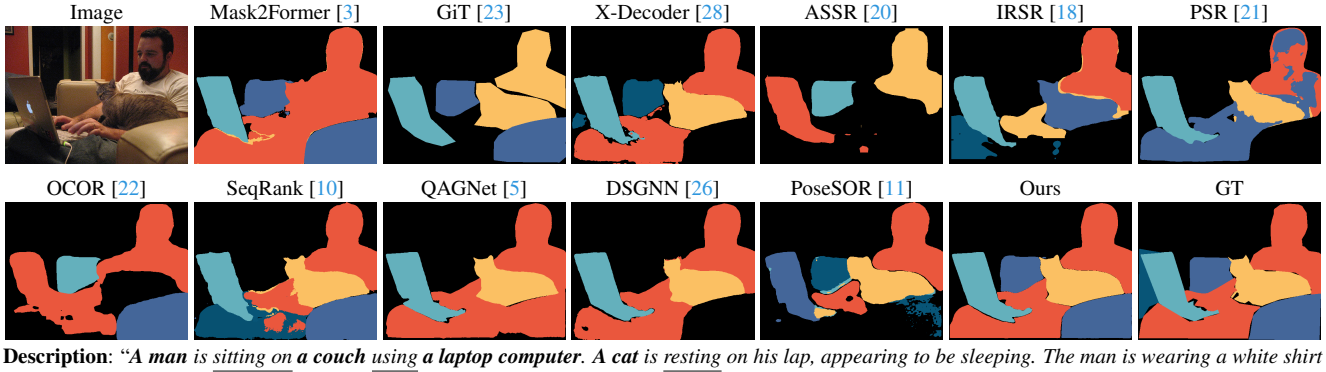

Description: "***A man*** *is sitting on* ***a couch*** *using* ***a laptop computer***. ***A cat*** *is resting on his lap, appearing to be sleeping. The man is wearing a white shirt and is typing on the laptop. The scene is cozy and relaxed, with the man and the cat ...*"

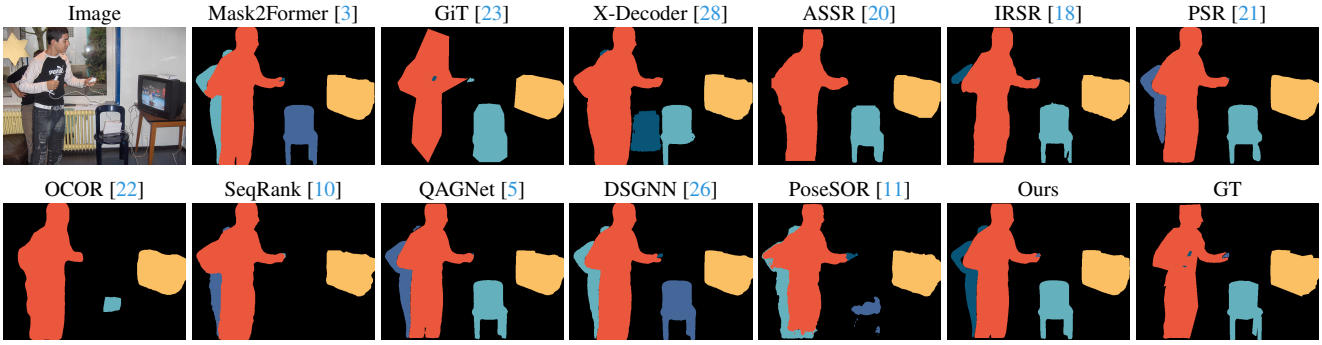

Description: "***A young man*** *is standing in a room, playing a video game on* ***a Nintendo Wii console***. *He is holding* ***a Wii remote***, *and the television screen displays the game he is playing. The room also features a couch, a chair, ...*"

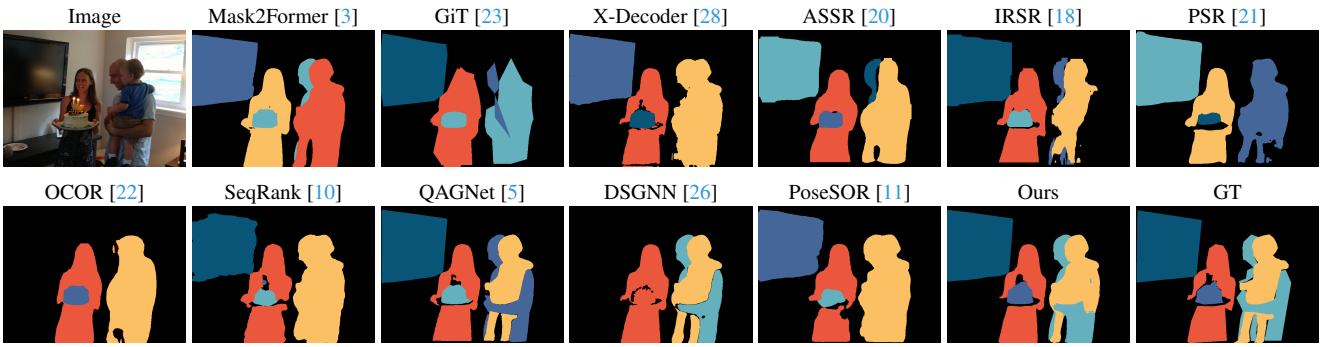

Description: "***A woman*** *is holding* ***a birthday cake with lit candles***, *and a man is holding* ***a baby***. *The woman is wearing a black dress and is smiling while presenting the cake. There are* ***a TV*** *on the wall ...*"

Figure A8. Qualitative comparison of our method with eleven best-performing methods in Table 1.